NANO LETTERS

2008
Vol. 8, No. 9
3056-3059

Doping Concentration of GaN Nanowires Determined by Opto-Electrical Measurements

T. Richter,* H. Lüth R. Meijers, R. Calarco, and M. Marso

Institute of Bio- and Nanosystems, IBN-1 and cni-Centre of Nanoelectronic Systems for Information Technology, Research Center Jülich, 52425 Jülich, Germany

Received May 19, 2008; Revised Manuscript Received July 7, 2008

ABSTRACT

The influence of n-doping on the electrical transport properties of GaN nanowires is investigated by photoconductivity measurements on wires with different diameters. The electrical transport in nanowires is extremely sensitive to the wire diameter because of the size dependent barrier for surface recombination. This effect is used to determine the doping level of the nanowires and to complete and consolidate our previously developed surface recombination model for GaN nanowires.

Introduction. Nanostructures such as semiconductor nanowires have attracted increasing interest as possible candidates for novel nanodevice concepts. One of the primary goals into this direction is focused on the fabrication of nanoelectronic devices and circuits by self-organized semiconductor whiskers growth.[1] This bottom up preparation technique yields alternatives or additional new pathways to fabrication in comparison to the standard well-established top-down methods of lithographic structuring of nanodevices. This is strongly motivated by the already proven high versatility and practical applications of nanowires in optical,[2,3] electrical,[4] chemical,[5] and biological devices.[6] Despite these promising achievements by researchers all over the world, there are still great challenges for future nanowire device applications such as the controlled n-doping of those nanoscale systems and its effect on the electrical transport.[7] To become feasible circuit elements, it is inescapable to find reliable and efficient techniques to dope these wires and analyze them efficiently.

In this work, we report the growth of n-doped (Si) GaN nanowires by plasma-assisted molecular beam epitaxy (MBE) on a Si(111) substrate. Size and density of the nanowires vary depending on the growth conditions, described elsewhere.[8] Ti/Au contacts patterned by electron beam lithography allow the electrical and optoelectrical characterization of the nanowires.[9] The electrical transport properties of the resulting metal−semiconductor−metal nanostructures are analyzed by means of current voltage measurements in the dark and under UV illumination, allowing the determination of the doping level.

Experimental Section. The GaN nanowires, both doped and nominally undoped, are grown by radio frequency plasma-assisted MBE on Si(111) under nitrogen rich condition. A detailed description of the growth optimization process for undoped nanowires can be found elsewhere.[8] The growth conditions for the samples studied in this work are presented in Table 1. The beam equivalent pressure (BEP) of Ga corresponds to $\Phi_{Ga} = 3.0 \times 10^{-8}$ mbar; the N_2 flux has been set to $\Phi_{N_2} = 4.0$ sccm, and the forward power of the radio frequency plasma cell has been set to $P_{RF} = 500$ W. The substrate temperature has been chosen to $T_{substrate} = 785$ °C. Si doping is carried out at a BEP of 0.6×10^{-9} mbar and 4.0×10^{-9} mbar to achieve different doping levels. Undoped and lightly doped nanowires have uniform diameter varying between 20 and 500 nm, whereas the highly doped wires show a broadening effect of the diameter along the axial direction (cf. Figure 1). After epitaxial growth, the nanowires are released from their native substrate, deposited on a Si(100) host substrate covered with a SiO_2 insulating layer, and are contacted by nonannealed Ti/Au ohmic electrodes[10] defined by electron beam lithography as described in ref 9 and shown in Figure 1D.

Table 1. Growth Parameters of GaN Nanowire Samples: Si-BEP and Deposition Time t_{dep}[a]

sample	Si BEP [$\times 10^{-9}$ mbar]	t_{dep} [min]	L [μm]
nominally undoped	0	360	1.0−1.2
lightly doped	0.6	240	0.8 < 1940.85
highly doped	4.0	240	1.0 < 1941.3

[a] The values of the column length L and the top-to-bottom ratio of the diameter, observed in SEM images (cf. Fig. 1), are also shown. For all of the samples, $\Phi_{Ga} = 3.0 \times 10^{-8}$ mbar, $T_{substrate} = 785$°C; a N_2 flux of 4.0 sccm and a plasma cell forward power of 500 W were used.

Results and Discussions. Cross-sectional SEM micrographs of the GaN nanowires are shown in Figure 1. In the

* Corresponding author.

10.1021/nl8014395 CCC: $40.75
Published on Web 08/08/2008

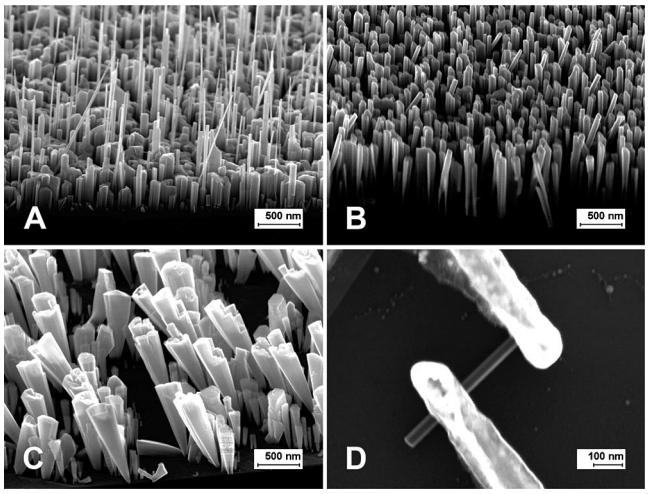

Figure 1. SEM images of the GaN nanowires. (A) Nominally undoped sample on native Si substrate. (B) Lightly doped sample on native Si substrate. (C) Highly doped sample on native Si substrate. (D) Single nanowire on host substrate, contacted by electron-beam lithography defined contacts.

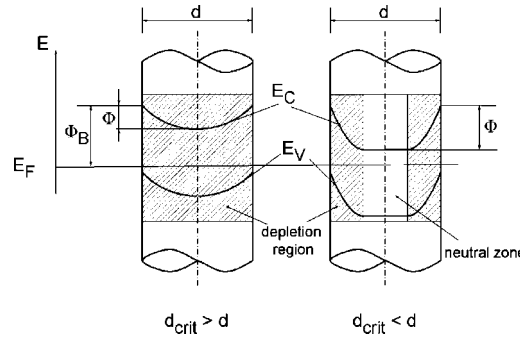

Figure 2. Surface depletion layer of GaN nanowires with the same diameter d but with different doping concentrations. The doping concentration of the left wire is lower than that for the right one. E is the electron energy; E_F is the Fermi level; E_C and E_V are conduction and valence band edges, respectively. ϕ is the recombination barrier, and ϕ_B is the Fermi level pinning position at the surface with respect to the Fermi level.

nominally undoped and lightly doped samples (Figure 1A,B), the wires grow vertically, with the *c* axis perpendicular to the substrate. In contrast, highly doped wires grown with high Si flux are often tilted, and the wire density is drastically reduced, as can be seen in the SEM image (Figure 1C). In addition, the wire morphology changes, giving rise to a diameter broadening from the bottom to the top. The ratio of the diameters at the top and those at the bottom is approximately 6 for the highly doped wires, in contrast to a ratio close to 1 for the samples grown with low and without Si flux. In addition, the top of the highly doped GaN nanowires often displays the formation of several new short wire-like structures (see Figure 1C), which also show a fairly well-developed hexagonal symmetry. In the following electrical and optoelectrical measurements on lightly and unintentionally doped wires, we chose to measure only wires with a tiny tapering effect, like the wire in Figure 1d, to minimize the error in the determination of the diameter. Furthermore, in all samples considered, the mean standard deviation in diameter amounts to ± 2.4 nm which results in an error of maximum 10% in the determination of the carrier concentration.

Electrical and optoelectrical measurements are performed to investigate the transport and intrinsic properties of the nanowires. The current through the GaN nanowires is not proportional to the cross section but shows a much stronger dependence due to the surface depletion region. Below a certain critical diameter d_{crit}, the wire is completely depleted and current flow is only possible with illumination by UV light. The photocurrent is extremely sensitive to wire diameter and doping concentration: the illuminated nanowire acts as a photoconductor, where the current generated by the incident photons is proportional to the lifetime of the photogenerated carriers. The carrier lifetime itself depends on the wire diameter, as explained below. The electric field of the surface depletion region drives the holes to the wire surface. The electrons, on the other hand, must overcome the potential barrier created by the depletion layer to recombine with the holes, if surface recombination is the main mechanism. This concept is described in detail in ref 9. For wire diameters above the critical diameter, the recombination barrier is defined by the surface Fermi-level pinning. For thinner wires, the depletion region is too small to build up such a large potential difference, and the recombination barrier is smaller. The smaller barrier yields a shorter lifetime of the photocarriers and therefore a lower photocurrent and a faster photoresponse. Below the critical diameter, the photocurrent shows an exponential dependence on diameter. For larger diameters, the dependence becomes linear. Increasing the doping concentration reduces the surface depletion layer thickness of the nanowire and the critical diameter, as shown in Figure 2. The determination of the critical diameter by electrical or optoelectrical measurements thus allows the evaluation of the doping concentration of the nanowire, as is shown below.

Current−voltage measurements with and without UV illumination are performed on nominally undoped and doped samples with different wire diameters. Illumination is performed with a mercury−xenon lamp via a quartz fiber (approximately 15 W/cm^2). Figure 3A shows the measurements of nanowires with thicknesses above their respective critical diameter, recognizable by a dark current well-above 1 nA at 1 V bias voltage. Nanowires with thicknesses below the critical diameter are completely depleted and show dark currents in the picoampere range, which is the resolution limit of our measurement setup. The dark current of the doped wires is higher than that of the undoped sample, although the diameter of the nominally undoped sample is 200 nm compared with 150 nm for the lightly doped one. The dark current of the highly doped sample with a diameter between 150 and 250 nm is so high that it masks the photocurrent of the illuminated device. The exact nominal diameters of the highly doped wires are difficult to define because of their conical shape.

The double logarithmic plot of the current under illumination as a function of the applied bias voltage shows the ohmic behavior (slope $m = 1$) at low voltages (up to 0.8 V) for all

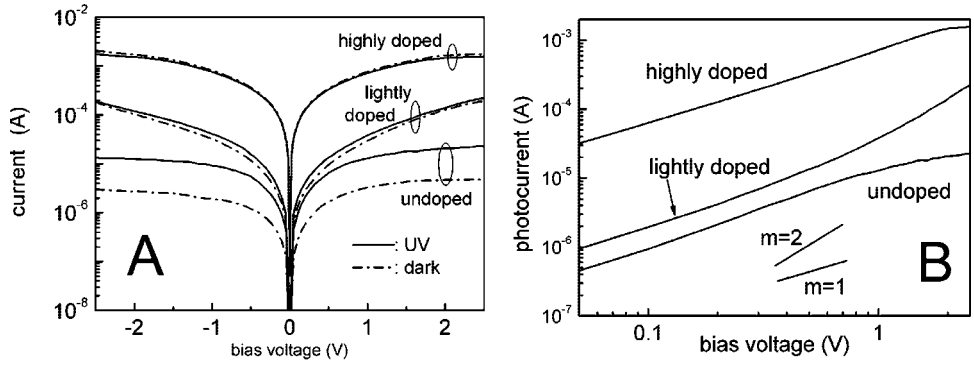

Figure 3. Current−voltage characteristics of different nanowires. Length between electrodes: 250 nm. Wire diameters: 200 nm (undoped), 150 nm (lightly doped), 150−250 nm (highly doped). (A) Measurement in the dark and with UV illumination. (B) Double logarithmic plot of the photocurrent.

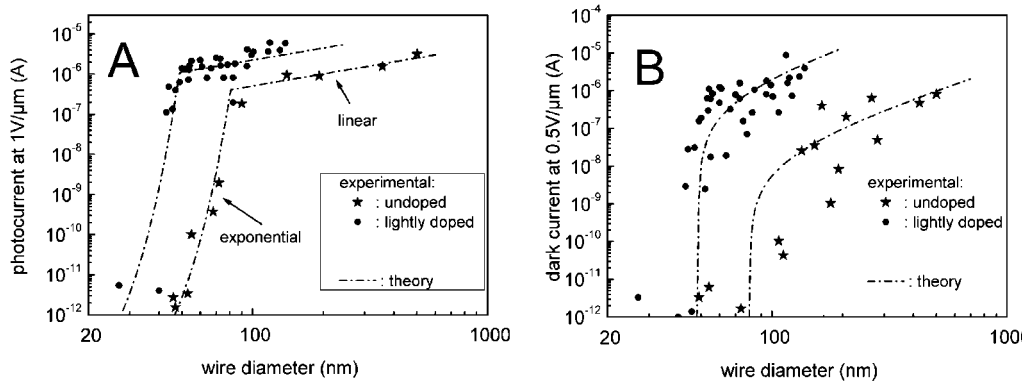

Figure 4. (A) Photocurrent versus wire diameter of the nominally undoped and lightly doped samples. The kink in the fitting curves indicates the critical diameter. (B) Dark current versus wire diameter of the nominally undoped and lightly doped samples. The fitting curves show an abrupt turn-on of the current when the wire diameter reaches d_{crit}.

three samples (Figure 3B). For higher voltages, the slope increases as an indication for space-charge-limited current.[11] We attribute the observed current saturation of the nominally undoped sample to the influence of the large contact resistance of the contact electrodes on the undoped GaN. The current saturation of the highly doped nanowire is also due to the effect of the contacts. In this case, the very high current flow compensates the much lower contact resistance.

Figure 4A shows the diameter dependence of the photocurrent of the undoped and lightly doped samples, for an applied bias of 1 V/μm wire length. The two different regions of exponential and linear dependence of the photocurrent as a function of diameter are clearly observable. The very high dark current of the highly doped sample hinders the accurate determination of the photocurrent. Furthermore, because of their conical shape, it is not possible to analyze them in the frame of a cylindrical approximation. The photocurrent of the lightly doped sample is higher than that for the nominally undoped one, and the region of exponential dependence is shifted toward lower diameters. This indicates a smaller critical diameter and therefore a higher doping concentration. The measurement data of both samples are fitted by the model presented in ref 9. This model provides three fitting parameters: the Fermi-level pinning ϕ_B, the doping concentration N_D, and a proportionality factor that includes the applied bias voltage, the illumination power, and details about the electron−hole pair generation mechanism. Fermi-level pinning is supposed to be independent of doping concentration. The extracted value for ϕ_B is 0.55 eV, in agreement to literature values.[12,13] The calculated doping concentrations are 6.25×10^{17} cm^{-3} and 1.8×10^{18} cm^{-3} for the nominally undoped and the lightly doped sample, respectively. For the doped sample, the carrier concentration nicely fits values which have been obtained for layers grown under comparable conditions.[14] The critical diameter at which the wire becomes depleted can be calculated by

$$d_{crit} = \sqrt{\frac{16\varepsilon \cdot \left(\Phi_B - kT \cdot \ln \frac{N_{eff}^L}{N_D}\right)}{q^2 \cdot N_D}}$$

where N_{eff}^L is the effective density of states in the conduction band, kT is 0.026 eV at room temperature, ε is the dielectric constant, and q is the elementary charge. The critical diameters are 81 and 49 nm for the nominally undoped and the lightly doped sample, respectively. The critical diameter d_{crit} can also be determined approximately by the kink between exponential and linear region of the measured diameter dependent photocurrent. Below the critical diameter, the photocurrent shows an exponential decrease, for larger diameters, it depends linearly on diameter.

The critical diameter and therefore the doping concentration could principally also be determined by dark current measurements as a function of diameter. If we suppose that

the thickness of the surface depletion region is independent of the diameter, then the dark current is proportional to $(d - d_{crit})^2$. A linear fit of the square root of the dark current would yield the critical diameter. However, the surface depletion region depends on the wire diameter, especially near the critical diameter. For an exact evaluation, the radius r_n of the neutral zone in the wire is calculated by the relation:[15]

$$\Phi = \Phi_B - kT \cdot \ln \frac{N_{eff}^L}{N_D} = -\frac{q^2 \cdot N_D}{4\varepsilon}\left(r_n^2 - \frac{d^2}{4} - 2r_n^2 \cdot \ln \frac{r_n}{d/2}\right)$$

In principle, this relation could be used to fit the dark current measurements by three fitting parameters N_D, ϕ_B, and a proportionality constant. However, the measurement points show a wider spread around the theoretical curve than for the photocurrent measurements. We attribute the stronger spread of the data points for dark current to the square dependence of the current on diameter, which enhances the error. Therefore, the photocurrent data should be preferred for an exact evaluation of the doping concentration. Figure 4B shows the measured dark current as a function of the wire diameter. The measurements are performed in the ohmic region of the current−voltage characteristics. For the calculated curves, we used the parameters N_D and ϕ_B determined by the photocurrent measurements. The proportionality factor that includes the bias voltage and the electron mobility is the only fitting parameter. The shape of the curves shows good agreement with the measured dark currents, especially the onset of the current flow that is identical with the critical diameter. This consistence between dark current and photocurrent behavior shows the validity of our model for current transport both in the dark and under illumination.

It should be noted that the determination of the carrier mobility by fitting of the dark current measurements is principally possible, but it gives an inaccuracy of 1 order of magnitude.

Conclusions. GaN nanowires with diameters between 30 nm and 600 nm are doped successfully by Si using plasma-assisted MBE. A high doping concentration changes the wire form to cones that grow upside down. Electrical and optoelectrical measurements are used to determine the doping concentration of nanowires that are contacted on a host substrate. Doping concentrations of 6.25×10^{17} cm^{-3} and 1.8×10^{18} cm^{-3} are derived for nominally undoped and n-doped samples, respectively.

The proposed characterization method uses the doping-dependence of the surface depletion layer thickness and its influence on the optoelectric current transport mechanism. It is an efficient and straightforward tool that can be used for nanowires of all materials where the surface level pinning creates a surface depletion layer. Hereby, a special advantage is that problems with contact resistances do not enter the quantitative analysis of the data.

Acknowledgment. The authors wish to thank K. H. Deussen and A. v.d. Hart for technical support.

References

(1) Duan, X.; Huang, Y.; Cui, Y.; Wang, J.; Lieber, C. M. *Nature* **2000**, *409*, 66.
(2) Kind, H.; Yan, H.; Messer, B.; Law, M.; Yang, P. *Adv. Mater.* **2002**, *14*, 158.
(3) Sirbuly, D. J.; Law, M.; Yan, H. Q.; Yang, P. D. *J. Phys. Chem. B* **2005**, *109*, 15190.
(4) Bryllert, T.; Wernersson, L.-E.; Lowgren, T.; Samuelson, L. *Nanotechnology* **2006**, *17*, 227.
(5) Chao, Li; Daihua, Zhang; Xiaolei, Liu; Song, Han; Tao, Tang; Jie, Han; Chongwu Zhou, *Appl. Phys. Lett.* **2003**, *82*, 1613.
(6) Cui, Y.; Wei, Q. Q.; Park, H.; Lieber, C. M. *Science* **2001**, *293*, 1289.
(7) Cui, Y.; Duan, X.; Hu, J.; Lieber, C. M. *J. Phys. Chem. B* **2000**, *104*, 5213.
(8) Meijers, R.; Richter, T.; Calarco, R.; Stoica, T.; Bochem, H.-P.; Marso, M.; Lüth, H. *J. Cryst. Growth* **2006**, *289*, 381.
(9) Calarco, R.; Marso, M.; Richter, T.; Aykanat, A. I.; Meijers, R.; van der Hart, A.; Stoica, T.; Lüth, H. *Nano Lett.* **2005**, *5*, 981.
(10) Schmitz, A. C.; Ping, A. T.; Khan, M. A.; Chen, Q.; Yang, J. W.; Adesicda, I. *Semicond. Sci. Technol.* **1996**, *11*, 1464.
(11) Rose, A. *Phys. Rev.* **1995**, *97*, 1538.
(12) Van de Walle, C. G.; Segev, D. *J. Appl. Phys.* **2007**, *101*, 081704.
(13) Koèan, M.; Rizzi, A.; Lüth, H; Keller, S; Mishra, U. K. *Phys. Status Solidi B* **1996**, *234*, 773.
(14) Sánchez-García, M. A.; Calleja, E.; Sanchez, F. J.; Calle, F.; Monroy, E.; Basak, D.; Muñoz, E.; Villar, C.; Sanz-Hervas, A.; Aguilar, M.; Serrano, J. J.; Blanco, J. M. *J. Electronic Mater. 27* **1998**, *4*, 276–281.
(15) Wegener, R. *IRE Transactions on Electron Devices* **1959**, *6*, 442.

NL8014395